
PER SUBJECT COMPLEXITY IN EYE MOVEMENT PREDICTION

Kateryna Melnyk *
Texas State University
San Marcos, Texas, 78640, USA
k_m825@txstate.edu

Dmytro Katrychuk
Texas State University
San Marcos, Texas, 78640, USA
d_k139@txstate.edu

Lee Friedman
Texas State University
San Marcos, Texas, 78640, USA
l_f96@txstate.edu

Oleg Komogortsev
Texas State University
San Marcos, Texas, 78640, USA
ok@txstate.edu

ABSTRACT

Eye movement prediction is a promising area of research to compensate for the latency introduced by eye-tracking systems in virtual reality devices. In this study, we comprehensively analyze the complexity of the eye movement prediction task associated with subjects. We use three fundamentally different models within the analysis: the lightweight Long Short-Term Memory network (LSTM), the transformer-based network for multivariate time series representation learning (TST), and the Oculomotor Plant Mathematical Model wrapped in the Kalman Filter framework (OPKF). Each solution is assessed following a sample-to-event evaluation strategy and employing the new event-to-subject metrics. Our results show that the different models maintained similar prediction performance trends pertaining to subjects. We refer to these outcomes as per-subject complexity since some subjects' data pose a more significant challenge for models. Along with the detailed correlation analysis, this report investigates the source of the per-subject complexity and discusses potential solutions to overcome it.

Keywords Eye Movement Prediction · Evaluation Metrics · Time-Series Forecasting · Oculomotor Plant Mathematical Model

1 Introduction

Millions of people worldwide are attracted and thrilled by the opportunity to participate in various entertainment activities, build new social connections, or experience immersive surroundings. The consumer tier of VR is growing, especially for graphically intensive environments with higher hardware requirements. VR headsets are across-the-board in usage within different areas such as training applications [1], healthcare in learning [2], or education [3]. Consumer-grade devices have resource constraints, and one of the technical issues is improving visual fidelity without raising the rendering cost in such demanding workloads [4].

The eye has a high visual acuity region known as a fovea. Visual sharpness decreases towards the periphery, first steeply and then more slowly. One performance optimization technique that utilizes this aspect of the Human Visual System (HVS) is Foveated Rendering (FR). It renders the image at a lower resolution in the periphery area but with high-quality graphics in the display area where the user is looking. Gaze-based FR requires an eye-tracking (ET) system to track real-time eye movement data at a particular frequency. The sampling frequency refers to how many times per second the eye-tracker measures eye movements.

FR is sensitive to the latency introduced by the ET system. If the system delay is high, the FR might render a full-resolution image in the former region of central vision. The acceptable value of system latency is below 40 ms [5, 6],

*corresponding author

which is not valid for most current head-mounted displays (HMDs) with integrated eye trackers [7]. Eye movement prediction helps make the FR more efficient and reduces latency by pre-rendering the content within the predicted future gaze area.

Researchers employ various strategies and algorithms to approach the eye movement prediction problem based on the selection of the input dataset because numerous data modalities are usually available after recording with VR devices. In published studies [8, 9, 10], they use head orientation data, positions of objects in the VR scene, and saliency maps, along with or without gaze data, to present a precise and efficient solution that could be lightweight enough to operate in real-time. The models used in the current study are trained on gaze vector data.

The validation and evaluation phases are crucial in any eye movement prediction framework, as eye-tracking data is naturally susceptible to various forms of noise introduced by participants and hardware and recording conditions. The main focus of the current work is to examine how model prediction performance varies from subject to subject. We present a more in-depth analysis of individual performance differences that can improve the eye movement prediction approaches. Our study addresses a critical gap in the existing literature by proposing and showing how to evaluate the model’s performance on a per-subject basis, as any solution should perform equally well for each individual to ensure that it accurately reflects personal variations in eye movement patterns. We introduce a set of event-to-subject metrics and show that a certain level of subject complexity associated with eye movement prediction errors remained constant for different models. We refer to the result as per-subject complexity since some participant data introduce varying challenges for the models during prediction. We analyze the sources of the per-subject trends in prediction performance through detailed correlation analysis and discuss potential solutions to enhance model generalizability across subjects.

2 Prior Work

2.1 Eye movement Prediction: Approaches

Over the past few years, visual attention and eye movement prediction have gained more and more academic interest. At first, researchers concentrated on identifying the areas or objects likely to attract the user’s attention in naturalistic scenarios. These models learned subject-dependent saliency maps and predicted fixation regions [11, 12]. Along with attention prediction, other groups focused on predicting the landing points of saccades. Different methods were utilized for making predictions: mathematical approaches based on ballistic characteristics of saccades [13, 14] or anatomically inspired Oculomotor Plant Mathematical Models (OPMMs) [15, 16]; deep learning approaches using Recurrent Neural Networks (RNNs) [17] and Long Short-Term Memory Networks (LSTM) [18, 19]. Positional data were typically used as input for landing point prediction. In solutions based on mathematical modeling, they were also used as the output. With deep learning approaches, predictions were made in various forms: gaze positions, the angle or direction of saccade movement, and saccade displacement.

With the advancement of eye-tracking technologies, the research direction changes to predicting the entire eye movement trajectory over time. The problem complexity is determined by the nature of the collected data and the horizon over which the gaze prediction is made. In many works, the horizon value was more than 150 ms [20, 9, 8]. The average latency for VR applications is under 30 ms. This makes shorter prediction horizons of 20 to 60 ms more relevant for real-time usage.

In a collection of studies, Hu and co-authors ([21, 8, 22, 9]) focused on the eye movement prediction problem. Each study provided a detailed correlation analysis of participants’ gaze and head movement data alongside VR content information such as task-related data, saliency maps, and object positions in dynamic scenes. In [8], the authors introduced a state-of-the-art (SotA) solution - DGaze. This CNN-based solution combines object positions in VR scenes, saliency maps, head velocity data, and, if available, users’ gaze positions (DGaze-ET) to predict future gaze data. In a subsequent study [9], a FixationNet model was introduced for forecasting human eye fixations within the task-oriented environment.

At the same time, one of the ongoing studies utilized RNN for eye movement prediction [10]. This work presented an LSTM-based architecture that uses head-mounted display (HMD) rotation and past gaze data. The transformers’ superior performance in many tasks has also triggered great interest within the eye-tracking community [23]. In [24], researchers worked on the gaze estimation and prediction pipeline. They tested several CNN architectures to find the most accurate gaze estimation solution. For the second part, they used estimated gaze vectors to predict gaze locations with an LSTM and Transformer architectures based on a self-attention mechanism. In [20], the authors experimented with the transformer-based model (GazeTransformer) that uses the gaze and IMU data as input. GazeTransformer was assessed using angular error over a 150 ms prediction interval (PI).

Some research groups have also formulated an eye movement prediction task as a sequential decision-making problem. Several works established Reinforcement Learning (RL) solutions that enhance human attention localization [25, 26, 27].

In [27], researchers showed the effectiveness of the RL approach in the driver gaze prediction domain, whereas in [25] study, the maximum entropy deep inverse RL model was demonstrated to be effective in the rear-end driving collision scenarios. Moreover, [28] introduce a transformer-based RL solution for predicting human gaze behavior during video viewing.

2.2 Eye movement Prediction: Evaluation and Metrics

A general range of metrics and visualization techniques is being commonly used for eye movement prediction. In most studies [10, 8, 20], the prediction error is calculated as the angular distance between the ground truth and the predicted gaze position expressed in degrees of visual angle (dva). The cumulative distribution function (CDF) plots were usually shown, with the x-axis representing prediction errors across the entire recording and the y-axis displaying the proportion of data. As a part of the analysis, the comparison tables showing prediction errors for different models and prediction intervals were included as well.

In [29], authors define multiple interesting metrics such as model consistency, partitioning error, overestimation, and underestimation rate for the time-to-event prediction. They highlight the idea that model evaluation needs to be done over different parts of time-to-saccade sequences to capture the overall prediction behavior. It is undoubtedly true that the aggregated prediction error over the entire recording may only partially represent the actual predictive performance of the model. An eye-tracking signal represents a sequence of various eye movement events: fixations, saccades, smooth pursuits, blinks, and microsaccades. Considering the characteristics of every event, some of them could be more or less challenging for the prediction algorithms. In [10] study, researchers illustrate the prediction errors at different normalized gaze velocities by dividing them into ten bins. The highest errors were observed when there was little gaze motion related to the gaze point, suggesting that the prediction of saccade landing points was more difficult.

In [30], the researchers emphasize the significance of the proper evaluation strategy inspecting the difficulties associated with eye movement signals. The authors propose the evaluation framework for the prediction task featuring a new metric called the Critical Evaluation Period (CEP). The metric creation was influenced by the phenomenon known as saccadic suppression. CEP was described as a 100 ms interval starting after the end of the saccade. The visualization of CEP prediction errors was done by dividing them into smaller subgroups according to the saccade amplitude values after which they occur. As demonstrated in that work [30], CEPs after saccades with larger amplitudes appeared more challenging for prediction algorithms.

Another critical phase of model evaluation is how signal quality impacts prediction performance. As it was shown in [10] study, assessing the model's performance on degraded signals reveals that the model can deal with lower-quality signals and perform well under less-than-ideal conditions.

3 Methodology

3.1 Prediction Models

3.1.1 LSTM

Based on the literature review, one of the most widely used deep learning architectures for the eye movement prediction problem was the LSTM model [24, 19, 10, 30]. Therefore, for the current study, we opted for a lightweight implementation consisting of two recurrent LSTM and two fully connected layers. The LSTM part had a hidden size of 32. The first fully connected layer consists of 32 nodes, and the second one has 16 nodes. For the model's detailed description, refer to [30] study.

3.1.2 TST

In the current study, we used the transformer-based architecture TSTPlus [31] to generalize the experiment results. We selected the Tsai library for implementation [32] as it was created specifically for time series tasks. The TST model consists of multiple encoder layers, and each encoder layer incorporates multi-head self-attention mechanisms. This design allows the model to capture temporal patterns by weighing the importance of different time steps in the input sequence. We used a custom head for this implementation. The custom head has the same structure as the baseline LSTM solution, consisting of two fully connected layers, with the first layer followed by a ReLU activation function. For the simplicity of comparison, we did not include hyperparameter tuning or experimentation with model parameters. We used the default set of parameters for the current results, which you can find in the package description [32].

3.1.3 OPKF

One of the most widely adopted anatomically inspired mathematical models of the oculomotor plant (OPMM) was introduced in 1980 [33]. Since that time, the model has established its practical use in various applications, including saccade simulation tailored on a per-subject level [34, 35], eye movement classification [36], biometrics research [37, 38], and gaze prediction [15, 16]. We included predictions made with the OPMM wrapped in the Kalman Filter framework (OPKF) to draw broad conclusions in our report.

A 13-parameter OPMM model was used with a slight modification made to the neural pulse calculation. The model parameters were estimated using the per-subject optimization procedure outlined in [35]. The Nelder-Mead optimization method was employed. The OPKF makes an initial guess by predicting an a priori estimate using the current state and a mathematical model. It then updates this prediction with the next available measurement (gaze position and velocity) for the observed part of the state. In simpler terms, at each time-step t , the OPKF receives an input consisting of the eye movement label and a state vector x^t , which includes the gaze position and velocity. It then outputs the predicted future gaze vector for time x^{t+PI} where PI - is the prediction interval.

3.2 Dataset

The current research used a subset of the “Gazebase Dataset” for its analysis and results. In eye movement prediction, this dataset has already been used in several studies for model evaluation [30, 10]. Refer to the “GazeBase” report [39] for a detailed overview of the database design, participants recruitment, tasks, stimuli descriptions, and all relevant details. All the recruited participants were undergraduate students from Texas State University. The dataset contains nine distinct ‘Rounds’ of data collected over a period of 37 months, with the largest sample population consisting of 322 subjects in Round 1. To be included in later rounds, subjects must have participated in all preceding rounds.

In this study, we employed Round 1 Session 1 of the random saccades task (RAN). The target was displaced at random locations across the monitor to induce visually guided oblique saccades with varying amplitudes. The displacements of the target ranged from $\pm 15^\circ$ and $\pm 9^\circ$ in the horizontal and vertical directions.

Ethics and Privacy Statement: All subjects provided informed consent following a protocol approved by the Institutional Research Board (IRB) at Texas State University prior to each round of recording. As part of the consent process, subjects acknowledged that their data may be shared in a de-identified form for research purposes. No subject-identifying information is included in the “GazeBase Dataset”.

3.3 Data Pre-processing

For OPKF prediction framework and evaluation purposes, we needed eye-tracking signals to be classified into eye movement events. An improved version of the MNH event classification algorithm [40] was employed. To execute a detailed analysis on a per-event and per-subject basis, a set of eye movement characteristics [41, 42] and signal quality measures [43, 44], such as spatial accuracy and precision, were calculated for each recording.

Each recording consists of time-series data, where the x and y components represent the horizontal and vertical gaze positions, measured in dva. For deep learning models, velocity data was used as input, and the displacement between gaze positions was used as output. For the OPKF model, gaze positional and velocity data, along with eye movement classification labels, are required. The model output is the predicted gaze position.

3.4 Training

The subjects were randomly split between the train and test datasets to reduce the risk of overfitting and ensure that models learn patterns that generalize well. We ended up with 255 subjects in the training dataset and 67 in the test dataset. The sliding window approach was used to train deep learning models, and the window length was set to 100 ms. The windows were shuffled before splitting into batches of size 256. To facilitate a smoother training process, the PyTorch Lightning framework [45] was applied. The loss function was defined as the mean Euclidean distance between the ground truth and predicted gaze data, and we utilized the Adam optimizer with a learning rate of 0.0003.

3.5 Evaluation and Metrics

As outlined in the "Prior Work" section, several standard metrics are widely used to evaluate eye movement prediction models. Following the established guidelines, this study will discuss both commonly used metrics and new ones that have proven helpful in our research.

3.5.1 Sample-to-Event Metrics

These metrics evaluate models either point-wise, considering the entire recording, or event-wise, considering the specific eye movement event in which the predicted horizon falls. The cumulative distribution function (CDF) of prediction errors when evaluating the overall signal, as well as fixation and saccade events separately, will be included in the analysis. We will also examine P_{95} error visualizations to understand how differently the models manage challenging conditions.

The CEP metric will also be included in our study, but it will be slightly modified. An active debate continues to be around the occurrence of saccadic suppression. It remains unclear how long it lasts before and after rapid eye movements. If we pull together the insights from the various studies, it can be concluded that saccadic suppression typically begins around 50 msec [46, 47] before the saccade and peaks at saccadic onset. It diminishes following a saccade and lasts for about 50-75 msec [48, 49]. In this study, in the 4th-row Figure 2, we partition the CEP visualization into two intervals and present the prediction results for the first 50 ms. This partition was chosen because our vision is still recovering during the first 50 ms but becomes sharp in the second half of CEP. Given the classification labels for the test dataset, we create the prediction error plots based on the amplitude of saccades.

3.5.2 Event-to-Subject Metrics

Previous research was more focused on analyzing the data complexity that arises from the nature of eye movement events, which leaves a gap in understanding the implications that come directly from the subjects. The various studies [34, 43, 42] examine and discuss the reliability of eye movement features, which are distinctive and temporally persistent for the same people over time. We calculated these features and aggregated them across participants to evaluate the person-specific effect on prediction performance.

We validate models on a broader scale to analyze errors at the per-subject level. Instead of looking at overall errors across the entire test set, we analyzed the median prediction error across all instances of the particular eye movement event for each subject individually. Let us consider a subject s with index e as an example for current analysis. Across the RAN task, s_e made around n fixations. We calculated P_{50} and P_{95} , resulting in two arrays of n errors for each model. Then, we calculate the median value for each of the two error arrays.

By aggregating the errors in this way, we can get a sense of how consistent the models’ predictions are across multiple occurrences of the same eye movement event for a subject and understand how the models’ predictions vary in more extreme cases. In this study, we used three distinct eye movement prediction algorithms. One of the primary objectives was to determine whether the performance of these solutions varies when applied to the same task for the same subjects.

4 Results

4.1 Sample-to-Event Analysis

This section explores the commonly used metrics for the eye movement prediction problem. In the first row of Figure 1, we present the CDF of prediction error across all the samples regardless of the eye movement classification. The y-value at any point on the CDF curve indicates the proportion of samples with errors less than or equal to the prediction error threshold on the x-axis. The error analysis using the full CDF metric does not represent a complete picture of the model’s performance. As the PI increases, it becomes difficult to distinguish between models with similar results.

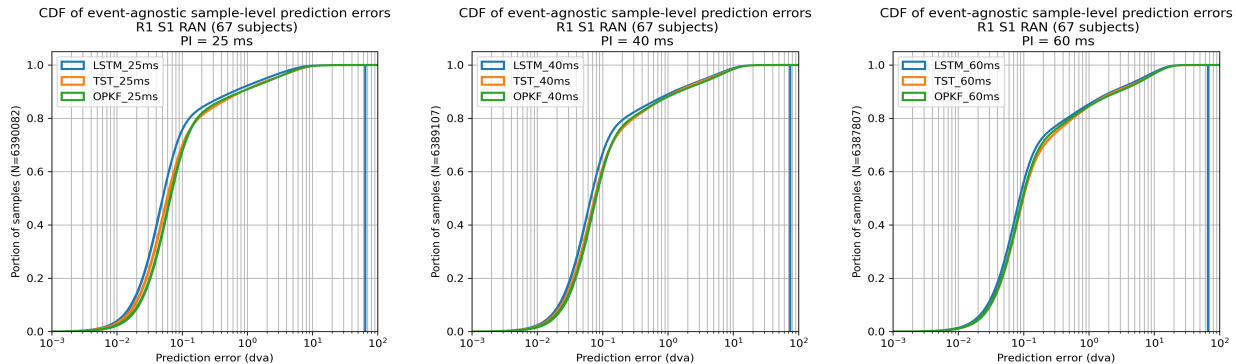


Figure 1: Per Sample-Wise Metric: CDF of event-agnostic prediction errors across different PIs

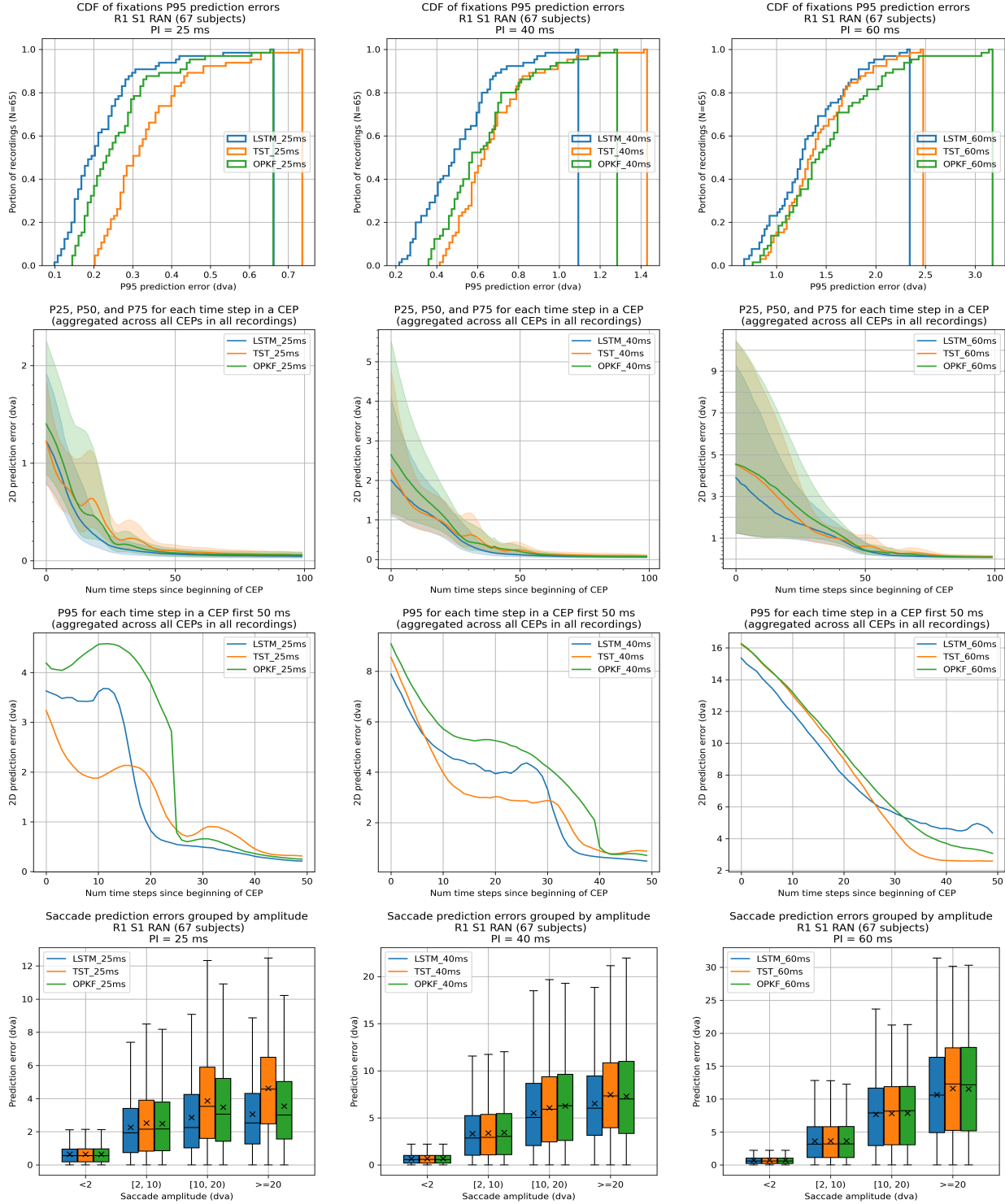


Figure 2: Sample-to-Event Metrics

In the first row of Figure 2, we explore the CDF of fixations P_{95} errors to understand how the model behaves in challenging parts of fixation events. A significant portion of them are recorded depending on the task. In this case, the average is around 80 – 90%. In the third row, we visualized the per-sample error for each timestamp in 100 ms of CEP. The next one presents the P_{95} per-sample error for the first 50 ms of CEP. This part of the analysis is crucial. The faster the model’s error converges to the stable point after a saccade, the greater the latency reduction would be allowed by the model’s prediction. The last row represents saccade prediction errors grouped by amplitude values. As in the saccade

landing point prediction, it is one of the most valuable measures as the more significant prediction errors are likely to be toward saccades with large amplitude values.

With this set of metrics, it is evident that the models fail to perform on average during certain eye movement events. However, whether the model is generalizable enough and if the average performance deviates across the specific subjects needs to be determined.

4.2 Event-to-Subject Analysis

We visualize the subject-specific metrics (see Figures 3, 4 and 5) for each model across three distinct prediction intervals (PIs). For each eye movement event, the top row represents P_{50} error, and the second row P_{95} . The plots need to be analyzed from left to right. We arranged them by PI value. The left-most plot represents errors for a 20 ms PI, the middle one a 40 ms PI, and the right one a 60 ms PI.

We observe similar prediction error behavior across three completely different models (see Figure 3). For example, the subject with an index 30 - S_{30} has the highest median P_{50} error during the fixation events across all PIs, and it posed the most significant challenge for all three models. However, the subject S_{25} has one of the lowest P_{50} errors. We can trace such a repetitive pattern throughout the entire test set of subjects.

Additionally, we calculate Kendall’s Coefficient of Concordance (KCC) [50] to check the correctness of the observation. KCC is a non-parametric measure used to assess the degree of agreement among raters. In our case, we can consider each model a rater and the median prediction error a degree of concordance. For each eye movement event, we present two tables of KCC values. In the left Tables (1a, 2a, 3a), we separately calculate KCC values across three PIs for each model. To explain the calculation using an example, assume we are analyzing the subject-wise P_{50} error for an LSTM model on fixation events. We calculated the error across three PIs and obtained three values for three different time points. We then compared the agreement in three LSTM predictions over time. We did the same for the other two models. In the right Tables (1b, 2b, 3b), we calculate KCC values across all models for each PI. Assume we are analyzing the subject-wise P_{95} error for the large saccade events. For the prediction interval of 60 ms, we had three distinct measures of P_{95} value from three prediction models. In this case, we measure the consistency of the models’ agreement per different PIs.

As we can see from Table 1 and Figure 3, the results are very consistent. The fixation error trend is stable per model level when the same model behavior is analyzed across three PIs and all KCC values exceed 0.9. Moreover, the pattern is consistent per PI level when the degree of agreement is calculated across the same PI for three completely different models.

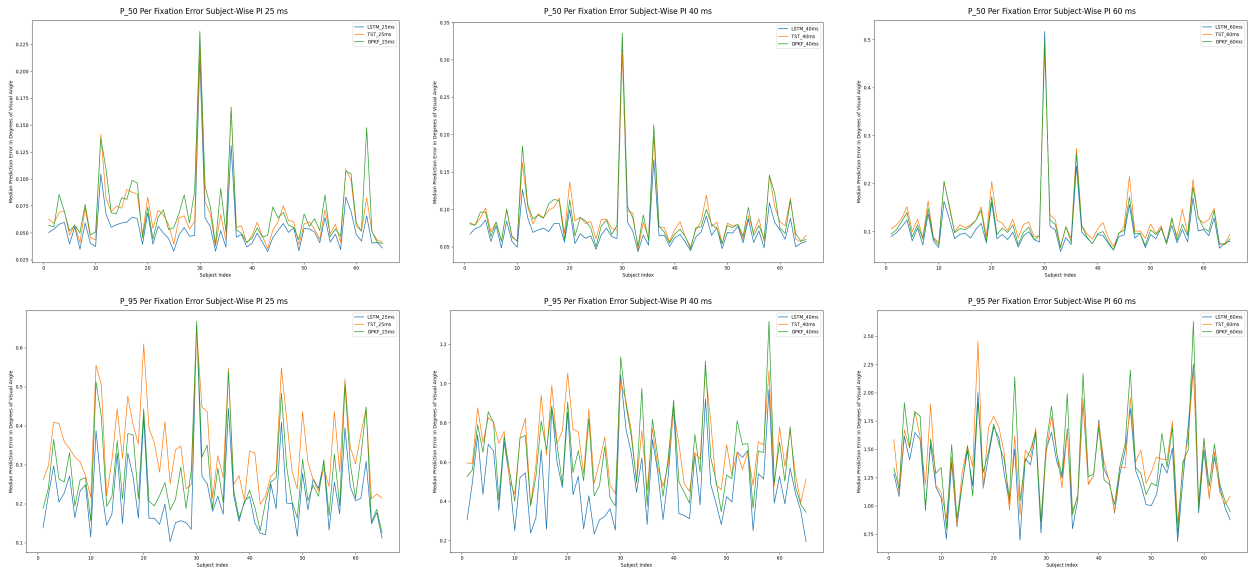


Figure 3: Event-to-Subject Metric for the Fixations

Model	P_{50}	P_{95}
LSTM	0.952	0.789
TST	0.925	0.771
OPKF	0.934	0.776

(a) Per Model Level of Agreement

PI	P_{50}	P_{95}
25	0.944	0.869
40	0.949	0.894
60	0.97	0.956

(b) Per PI Level of Agreement

Table 1: KCC Values Fixation

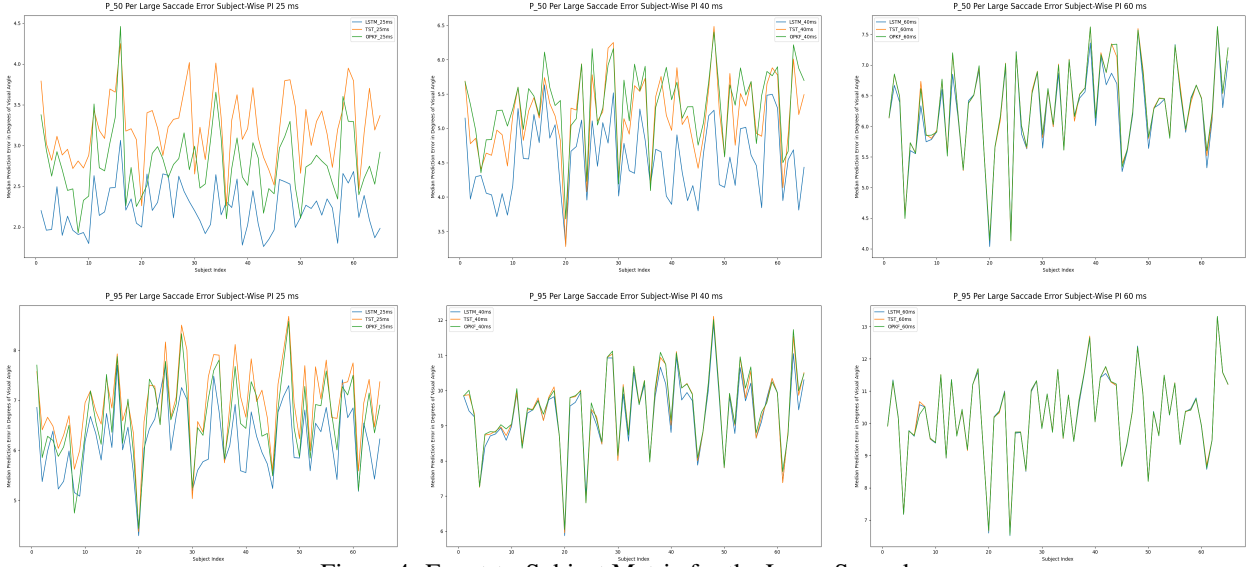


Figure 4: Event-to-Subject Metric for the Large Saccades

We got somewhat different results for the large saccades (see Figure 4). The pattern was not consistent for the 40 ms PI. However, we observe that the trend becomes more stable with the increase in the PI value. The large saccade error pattern was not repetitive per model level. In other words, the most challenged subject within the 25 ms PI was not the most challenging per 40 and 60 ms PIs. However, the subject with index 20 appeared to have the lowest median P_{95} error, and the same was true for the P_{50} error 60 ms PI.

Table 2: KCC values Large Saccades

Model	p_50	p_95
LSTM	0.584	0.649
TST	0.715	0.782
OPKF	0.621	0.742

(a) Per Model Level of Agreement

PI	p_50	p_95
25	0.763	0.929
40	0.828	0.988
60	0.993	0.999

(b) Per PI Level of Agreement

In Table 2, KCC values confirm our observations. The LSTM model is the most inconsistent in its behavior across three PIs, compared to the other models used in the study. However, the numbers are still relatively high when discussing the degree of agreement among models.

We can see that each model is consistent in its results for the small saccades, and their performance is very close (Figure 5 and Table 3). We observed that the complexity varied per event depending on the subjects. Some subjects had more challenging fixation regions, while others had more complex saccadic events for prediction. Moreover, there is a clear distinction in the complexity of predicting large and small saccades for the same people.

All three algorithms use fundamentally different approaches to learning from train data. However, they achieve roughly the same median prediction accuracy for each test subject. Upon receiving these results, we became interested in investigating the question: "Where does this subject complexity come from?" Since we have yet to see in the literature that somebody reported such insights for any prediction models.

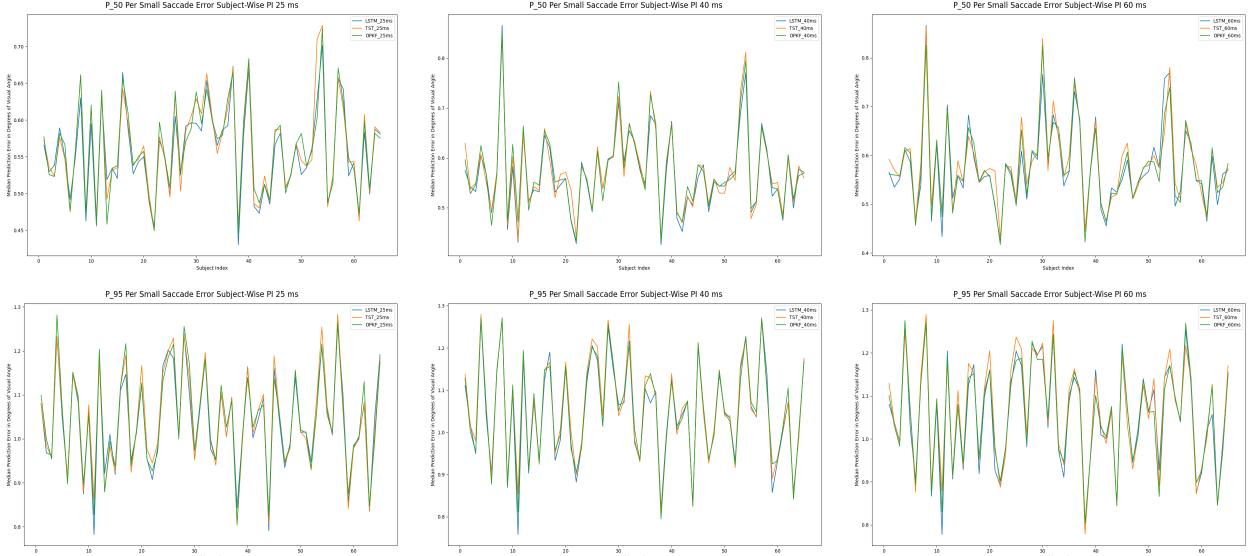


Figure 5: Event-to-Subject Metric for the Small Saccades

Table 3: KCC values Small Saccades

Model	p_50	p_95
LSTM	0.968	0.955
TST	0.943	0.951
OPKF	0.962	0.958

(a) Per Model Level of Agreement

PI	p_50	p_95
25	0.982	0.989
40	0.982	0.993
60	0.968	0.988

(b) Per PI Level of Agreement

4.3 What Causes Variation in Complexity Across Different Subjects?

The logical assumption will be that complexity arises from the distinctive patterns of eye movement events. For example, the difficulty of making predictions across fixation regions may be caused by its trajectory’s inconsistent shape or unpredictable behavior [41]. The difficulty associated with the saccades can originate from the desynchronization of its vertical and horizontal channels [51]. We performed a detailed correlation analysis to shed light on what specific characteristic leads to this prediction behavior. We computed the following set of features:

- six descriptive statistical measures were calculated from each of 25 fixation and 52 saccade characteristics, resulting in a total of 462 features[42];
- 128-dimensional embeddings computed by deep-learning based model "Eye know you too" [52];
- 2 signal quality measures per subject recording [44], and 5 distinct noise related measures [40].

Since the data in the analysis does not follow a normal distribution, we reported the Spearman correlation coefficients within the study. This section presents two tables: one with the correlation results for the fixations and another for the large saccade events. We exclude the table for small saccades, as there are no correlation scores between the median prediction errors and their features more significant than the 0.3 value. However, we found some characteristics highly correlated with the median fixation and large saccade prediction errors.

One of the most highly correlated features with the per-subject P_{50} errors (see Table 4) was the fixation radial velocity profile mean/median values (F_{14} - F_{15} features in [42]). The low-velocity values characterize fixation eye movements. Our results show increased prediction error when the average fixation velocity is high per participant. On the other hand, the fixation drift feature, which correlated well with the P_{95} error, can provide information about visual input stability in the subject’s retina (F_{06} feature in [42]). It can also be helpful in the inspection of the quality of the eye-tracking signal.

Since both measures relate to the noise that may be present in the data, we added characteristics that describe its different levels within the eye-tracking signal. The fixation noise threshold is one the most strongly related features to P_{50} errors (see Table 5). The full feature description can be found in the MNH study (p.1378, [40]). It is calculated by combining the velocities from the fixation blocks that are likely to be the most stable and taking from them the 90th percentile of the velocity noise distribution. None of the noise characteristics were highly related to the small or large saccade features.

(a) PI 25 ms

Model	P_q	Feature	Spearman	P_q	Feature	Spearman
LSTM	P_{50}	VelProfMd_R_Md	0.85	P_{95}	DriftAvgSpeed_R_Md	0.81
TST	P_{50}	VelProfMd_R_Md	0.89	P_{95}	Dur_Sk	0.79
OPKF	P_{50}	VelProfMd_R_Md	0.87	P_{95}	DriftAvgSpeed_R_Md	0.77

(b) PI 40 ms

Model	P_q	Feature	Spearman	P_q	Feature	Spearman
LSTM	P_{50}	VelProfMn_R_Md	0.72	P_{95}	DriftAvgSpeed_R_Md	0.77
TST	P_{50}	VelProfMn_R_Md	0.76	P_{95}	Dur_Sk	0.77
OPKF	P_{50}	VelProfMn_R_Md	0.9	P_{95}	DriftAvgSpeed_R_Md	0.76

(c) PI 60 ms

Model	P_q	Feature	Spearman	P_q	Feature	Spearman
LSTM	P_{50}	DriftAvgSpeed_R_Md	0.77	P_{95}	DriftAvgSpeed_R_Md	0.5
TST	P_{50}	DriftAvgSpeed_R_Md	0.74	P_{95}	DriftAvgSpeed_R_Md	0.47
OPKF	P_{50}	DriftAvgSpeed_R_Md	0.76	P_{95}	DriftAvgSpeed_R_Md	0.57

Table 4: Correlation Analysis: P_{50} & P_{95} Per-Subject Wise Prediction Errors and Fixation Characteristics

Feature	Model	P_q	PI	Spearman	PI	Spearman	PI	Spearman
FixNoiseThr	LSTM	P_{50}	25	0.88	40	0.79	60	0.73
FixNoiseThr	TST	P_{50}	25	0.92	40	0.85	60	0.76
FixNoiseThr	OPKF	P_{50}	25	0.88	40	0.93	60	0.83

Table 5: Correlation Analysis: P_{50} & P_{95} Per-Subject Wise Prediction Errors and Fixation Characteristics

For the saccades per-subject P_{50} error of the LSTM model, we have found a significant relationship with the median value of the acceleration profile (S_{30} feature in [42]). It indicates that making predictions with the current model was more difficult for people whose saccade speed changes quickly. The correlation coefficient was also high between the P_{95} error and the median value of the peak velocity duration ratio (S_{03} feature in [42]). The ratio feature exhibits a high correlation in one of the studies with the human level of alertness [53].

In Table 6, it is visible that the correlation coefficients change with the PI value. The smaller the PI, the more likely the models will learn an individual pattern related to large saccadic events. Despite the most significant consistency among small saccades and model predictions, no characteristics correlate with their median prediction errors. Another observation was that the embeddings were not among the highly correlated features for prediction errors.

5 Discussion

This study illustrates the impact of subject complexity on the eye movement prediction problem. We introduce new event-to-subject metrics based on the existing sample-to-sample and sample-to-event measures for broader analysis. With a fresh angle of data exploration, we notice that different models follow the matching prediction error trends for the test dataset. We examine relationships between the median per subject prediction errors and varied measures that characterize each recording.

We use 462 descriptive statistics features calculated over the values from the instances of fixation and saccades, 128 biometric embeddings, five noise-related measures, and two signal quality measures for correlation analysis. The highest correlation coefficients we get are for the fixation per-subject errors. The fixations account for more than 80% of the recording on average, and the value of personal noise has the most influence on the prediction performance. Based on correlation analysis, the coefficients decrease as the PI increases; however, their values remain high. The data shows that the models are more noise-sensitive at a shorter PI.

Given that the prediction per-subject error trends for small saccades are even more persistent, we do not find measures to explain this consistency among the explored characteristics. Small saccades are generally problematic parts for signal prediction. The models used in the current study forecast them equally poorly. This difficulty is natural because they are small, less than 2 degrees, and predictive models can not adapt to such short events. The level of agreement among models per PI is high for the large saccades, but the error trend per each model separately across all PIs is

(a) PI 25 ms

Model	P_q	Feature	Spearman	P_q	Feature	Spearman
LSTM	P_{50}	AccProfMd_R_Md	0.81	P_{95}	PkVelDur_Ratio_R_Md	0.9
TST	P_{50}	PkAcc_R_Md	0.66	P_{95}	PkVelDur_Ratio_R_Md	0.68
OPKF	P_{50}	PkVelDur_Ratio_R_Md	0.59	P_{95}	PkVelDur_Ratio_R_Md	0.75

(b) PI 40 ms

Model	P_q	Feature	Spearman	P_q	Feature	Spearman
LSTM	P_{50}	PkVelDur_Ratio_R_Md	0.75	P_{95}	AmpDur_Ratio_R_Md	0.49
TST	P_{50}	MnVel_R_Md	0.65	P_{95}	AmpDur_Ratio_R_Md	0.43
OPKF	P_{50}	PkVelDur_Ratio_R_Md	0.59	P_{95}	AmpDur_Ratio_R_Md	0.43

(c) PI 60 ms

Model	P_q	Feature	Spearman	P_q	Feature	Spearman
LSTM	P_{50}	PkVelMnVel_Ratio_H_Md	-0.29	P_{95}	VelProfSk_R_Md	-0.4
TST	P_{50}	PkVelMnVel_Ratio_H_Md	-0.26	P_{95}	VelProfSk_R_Md	-0.41
OPKF	P_{50}	VelProfSk_R_Md	-0.26	P_{95}	VelProfSk_R_Md	-0.41

Table 6: Correlation Analysis: P_{50} & P_{95} Per-Subject Wise Prediction Errors and Saccade Characteristics

less consistent. Correlation results indicate that people with higher median saccade speeds are more challenging for prediction algorithms.

After analysis, we want to discuss a couple of points. Data selection is a vital factor influencing the subject’s effect on the model’s performance. In the present study, we employ high-quality eye-tracking data collected using an EyeLink 1000 eye tracker, where the noise level is generally low. OPKF can work with any quality signal by its design, even if irregularities occur in real-time. Its prediction performance will likely remain consistent across test subjects at the different PIs. However, for the deep learning models, the higher presence of noise poses more challenges during the real-time prediction. Therefore, whether models trained and tested on lower-quality data demonstrate persistent performance across event-to-subject measures is worth investigating.

Another critical point to mention is that the goal of any prediction algorithm is to achieve unbiased results across a set of subjects. In the current study, we utilize only gaze vectors without additional data. The SotA solutions described in the literature review use multiple data streams. In cases when researchers used the head-movement data, the difference in model performance between subjects could be even more significant. In some studies [8, 9], the researchers explored the gaze-head correlation in dynamic scenes and reported the strong relationship between the users’ gaze positions and head rotation velocities, which can potentially lead to a more significant effect of the personal noise on the model’s predictions. Hence, it should be an essential part of the evaluation phase of the eye-movement prediction problem to check if the model performs consistently well for all subjects to avoid bias toward specific individuals.

We aim to focus more on deep learning solutions, and we will consider strategies to improve their performance and generalizability across subjects. One idea is to apply subject-specific information during the training phase. For example, we can incorporate eye movement features alongside gaze data as inputs to the model, or we can use embeddings to help the solution leverage patterns learned in end-to-end manner. For future experiments, we will test the new model on data recorded with the VR device to compare it with the SotA. One technique that could be applied is domain adaptation for time-series forecasting. We still plan to use the gaze vector data as input and shorter PIs, and with the proper model setup, we can fine-tune the new model for the VR dataset when it was initially trained on the gaze data from the GaseBase dataset. In summary, since we have yet to see in the literature that somebody reported such per-subject performance for any prediction models, it is a significant part of the evaluation that deserves closer attention.

6 Conclusion

This study analyzes the complexity of the eye movement prediction problem associated with subjects’ data. We use three fundamentally different models to create a fair comparison and show the relevance of the results. We noted the consistency in eye movement prediction performance across the same test subjects with the new event-to-subject measures. We assessed the validity of all observations by calculating Kendall’s Coefficient of Concordance to measure the level of agreement among the predictive algorithms across three different PIs.

We conducted a correlation analysis between various eye movement features and median per-subject errors to examine the source of the model’s consistent prediction behavior. Since we found that even high-quality data can be significantly affected by the personal noise level or subjects-specific eye movement patterns, it is crucial to prioritize model generalizability across subjects during the evaluation phase of any eye movement prediction study and integrate measures into the analysis that can reveal it.

References

- [1] Biao Xie, Huimin Liu, Rawan Alghofaili, Yongqi Zhang, Yeling Jiang, Flavio Destri Lobo, Changyang Li, Wanwan Li, Haikun Huang, Mesut Akdere, et al. A review on virtual reality skill training applications. *Frontiers in Virtual Reality*, 2:645153, 2021.
- [2] Henna Mäkinen, Elina Haavisto, Sara Havola, and Jaana-Maija Koivisto. User experiences of virtual reality technologies for healthcare in learning: an integrative review. *Behaviour & Information Technology*, 41(1):1–17, 2022.
- [3] Laura Freina and Michela Ott. A literature review on immersive virtual reality in education: state of the art and perspectives. In *The international scientific conference elearning and software for education*, volume 1, pages 10–1007, 2015.
- [4] Sage L Matthews, Alvaro Uribe-Quevedo, and Alexander Theodorou. Rendering optimizations for virtual reality using eye-tracking. In *2020 22nd symposium on virtual and augmented reality (SVR)*, pages 398–405. IEEE, 2020.
- [5] Rachel Albert, Anjul Patney, David Luebke, and Joohwan Kim. Latency requirements for foveated rendering in virtual reality. *ACM Transactions on Applied Perception (TAP)*, 14(4):1–13, 2017.
- [6] Jan-Philipp Stauffert, Florian Niebling, and Marc Erich Latoschik. Latency and cybersickness: Impact, causes, and measures. a review. *Frontiers in Virtual Reality*, 1:582204, 2020.
- [7] Niklas Stein, Diederick C Niehorster, Tamara Watson, Frank Steinicke, Katharina Rifai, Siegfried Wahl, and Markus Lappe. A comparison of eye tracking latencies among several commercial head-mounted displays. *i-Perception*, 12(1):2041669520983338, 2021.
- [8] Zhiming Hu, Sheng Li, Congyi Zhang, Kangrui Yi, Guoping Wang, and Dinesh Manocha. Dgaze: Cnn-based gaze prediction in dynamic scenes. *IEEE transactions on visualization and computer graphics*, 26(5):1902–1911, 2020.
- [9] Zhiming Hu, Andreas Bulling, Sheng Li, and Guoping Wang. Fixationnet: Forecasting eye fixations in task-oriented virtual environments. *IEEE Transactions on Visualization and Computer Graphics*, 27(5):2681–2690, 2021.
- [10] Gazi Karam Illahi, Matti Siekkinen, Teemu Kämäräinen, and Antti Ylä-Jääski. Real-time gaze prediction in virtual reality. In *Proceedings of the 14th international workshop on immersive mixed and virtual environment systems*, pages 12–18, 2022.
- [11] Eunji Chong, Nataniel Ruiz, Yongxin Wang, Yun Zhang, Agata Rozga, and James M Rehg. Connecting gaze, scene, and attention: Generalized attention estimation via joint modeling of gaze and scene saliency. In *Proceedings of the European conference on computer vision (ECCV)*, pages 383–398, 2018.
- [12] Marcella Cornia, Lorenzo Baraldi, Giuseppe Serra, and Rita Cucchiara. Sam: Pushing the limits of saliency prediction models. In *Proceedings of the IEEE Conference on Computer Vision and Pattern Recognition Workshops*, pages 1890–1892, 2018.
- [13] Céline Paeye, Alexander C Schütz, and Karl R Gegenfurtner. Visual reinforcement shapes eye movements in visual search. *Journal of vision*, 16(10):15–15, 2016.
- [14] Elena Arabadzhiyska, Okan Tarhan Tursun, Karol Myszkowski, Hans-Peter Seidel, and Piotr Didyk. Saccade landing position prediction for gaze-contingent rendering. *ACM Transactions on Graphics (TOG)*, 36(4):1–12, 2017.
- [15] Oleg V Komogortsev and Javed I Khan. Eye movement prediction by kalman filter with integrated linear horizontal oculomotor plant mechanical model. In *Proceedings of the 2008 symposium on Eye tracking research & applications*, pages 229–236, 2008.
- [16] Oleg V Komogortsev and Javed I Khan. Eye movement prediction by oculomotor plant kalman filter with brainstem control. *Journal of Control Theory and Applications*, 7:14–22, 2009.
- [17] Aythami Morales, Francisco M Costela, Ruben Tolosana, and Russell L Woods. Saccade landing point prediction: A novel approach based on recurrent neural networks. In *Proceedings of the 2018 International Conference on Machine Learning Technologies*, pages 1–5, 2018.

- [18] Henry Griffith and Oleg Komogortsev. A shift-based data augmentation strategy for improving saccade landing point prediction. In *ACM Symposium on Eye Tracking Research and Applications*, pages 1–6, 2020.
- [19] Aythami Morales, Francisco M Costela, and Russell L Woods. Saccade landing point prediction based on fine-grained learning method. *IEEE Access*, 9:52474–52484, 2021.
- [20] Tim Rolff, H Matthias Harms, Frank Steinicke, and Simone Frintrop. Gazetransformer: Gaze forecasting for virtual reality using transformer networks. In *DAGM German Conference on Pattern Recognition*, pages 577–593. Springer, 2022.
- [21] Zhiming Hu, Congyi Zhang, Sheng Li, Guoping Wang, and Dinesh Manocha. Sgaze: A data-driven eye-head coordination model for realtime gaze prediction. *IEEE transactions on visualization and computer graphics*, 25(5):2002–2010, 2019.
- [22] Zhiming Hu. Gaze analysis and prediction in virtual reality. In *2020 IEEE conference on virtual reality and 3D user interfaces abstracts and workshops (VRW)*, pages 543–544. IEEE, 2020.
- [23] Qingsong Wen, Tian Zhou, Chaoli Zhang, Weiqi Chen, Ziqing Ma, Junchi Yan, and Liang Sun. Transformers in time series: A survey. *arXiv preprint arXiv:2202.07125*, 2022.
- [24] Pier Luigi Mazzeo, Dilan D’Amico, Paolo Spagnolo, and Cosimo Distanto. Deep learning based eye gaze estimation and prediction. In *2021 6th International Conference on Smart and Sustainable Technologies (SpliTech)*, pages 1–6. IEEE, 2021.
- [25] Sonia Bae, Erfan Pakdamanian, Inki Kim, Lu Feng, Vicente Ordonez, and Laura Barnes. Medirl: Predicting the visual attention of drivers via maximum entropy deep inverse reinforcement learning. In *Proceedings of the IEEE/CVF international conference on computer vision*, pages 13178–13188, 2021.
- [26] Zhibo Yang, Lihan Huang, Yupei Chen, Zijun Wei, Seoyoung Ahn, Gregory Zelinsky, Dimitris Samaras, and Minh Hoai. Predicting goal-directed human attention using inverse reinforcement learning. In *Proceedings of the IEEE/CVF conference on computer vision and pattern recognition*, pages 193–202, 2020.
- [27] Kai Lv, Hao Sheng, Zhang Xiong, Wei Li, and Liang Zheng. Improving driver gaze prediction with reinforced attention. *IEEE Transactions on Multimedia*, 23:4198–4207, 2020.
- [28] Süleyman Özdel, Yao Rong, Berat Mert Albaba, Yen-Ling Kuo, Xi Wang, and Enkelejda Kasneci. A transformer-based model for the prediction of human gaze behavior on videos. In *Proceedings of the 2024 Symposium on Eye Tracking Research and Applications*, pages 1–6, 2024.
- [29] Tim Rolff, Niklas Stein, Markus Lappe, Frank Steinicke, and Simone Frintrop. Metrics for time-to-event prediction of gaze events. In *NeuRIPS 2022 Workshop on Gaze Meets ML*, 2022.
- [30] Samantha Aziz, Dillon J Lohr, Razvan Stefanescu, and Oleg Komogortsev. Practical perception-based evaluation of gaze prediction for gaze contingent rendering. *Proceedings of the ACM on Human-Computer Interaction*, 7(ETRA):1–17, 2023.
- [31] George Zerveas, Srideepika Jayaraman, Dhaval Patel, Anuradha Bhamidipaty, and Carsten Eickhoff. A transformer-based framework for multivariate time series representation learning. In *Proceedings of the 27th ACM SIGKDD conference on knowledge discovery & data mining*, KDD ’21, page 2114–2124, New York, NY, USA, 2021. Association for Computing Machinery.
- [32] Ignacio Oguiza. tsai - a state-of-the-art deep learning library for time series and sequential data. Github, 2023.
- [33] A Terry Bahill. Development, validation and sensitivity analyses of human eye movement models. *CRC Critical Reviews in Bioengineering*, 4(4):311–355, 1980.
- [34] Kateryna Melnyk, Lee Friedman, Dmytro Katrychuk, and Oleg Komogortsev. Per-subject oculomotor plant mathematical models and the reliability of their parameters. *Proceedings of the ACM on Computer Graphics and Interactive Techniques*, 7(2):1–20, 2024.
- [35] Dmytro Katrychuk and Oleg V. Komogortsev. A study on the generalizability of oculomotor plant mathematical model. In *2022 Symposium on Eye Tracking Research and Applications*, ETRA ’22, New York, NY, USA, 2022. Association for Computing Machinery.
- [36] Federico Wadehn, David J Mack, Thilo Weber, and Hans-Andrea Loeliger. Estimation of neural inputs and detection of saccades and smooth pursuit eye movements by sparse bayesian learning. In *2018 40th Annual International Conference of the IEEE Engineering in Medicine and Biology Society (EMBC)*, volume 2018, pages 2619–2622. IEEE, 04 2018.
- [37] Oleg Komogortsev, Sampath Jayarathna, Cecilia Aragon, and Mechehouh Mahmoud. Biometric identification via an oculomotor plant mathematical model. In *Proceedings of the 2010 Symposium on Eye-Tracking Research & Applications*, ETRA ’10, page 57–60, New York, NY, USA, 01 2010. Association for Computing Machinery.

- [38] Oleg Komogortsev, Cecilia Aragon, Alexey Karpov, and Larry Price. Biometric authentication via oculomotor plant characteristics. *IEEE/IARP International Conference on Biometrics (ICB)*, pages 413–420, 04 2012.
- [39] Henry Griffith, Dillon Lohr, Evgeny Abdulin, and Oleg Komogortsev. Gazebase, a large-scale, multi-stimulus, longitudinal eye movement dataset. *Scientific Data*, 8(1):184, 07 2021.
- [40] Lee Friedman, Ioannis Rigas, Evgeny Abdulin, and Oleg V Komogortsev. A novel evaluation of two related and two independent algorithms for eye movement classification during reading. *Behavior Research Methods*, 50:1374–1397, 05 2018.
- [41] Kateryna Melnyk, Lee Friedman, and Oleg V Komogortsev. What can entropy metrics tell us about the characteristics of ocular fixation trajectories? *Plos one*, 19(1):e0291823, 2024.
- [42] Ioannis Rigas, Lee Friedman, and Oleg Komogortsev. Study of an extensive set of eye movement features: Extraction methods and statistical analysis. *Journal of Eye Movement Research*, 11(1), 2018.
- [43] Mehedi Hasan Raju, Lee Friedman, Dillon J Lohr, and Oleg V Komogortsev. Temporal persistence and inter-correlation of embeddings learned by an end-to-end deep learning eye movement-driven biometrics pipeline, 2024.
- [44] Dillon J. Lohr, Lee Friedman, and Oleg V. Komogortsev. Evaluating the data quality of eye tracking signals from a virtual reality system: Case study using smi’s eye-tracking htc vive, 2019.
- [45] William Falcon. Pytorch lightning, March 2019.
- [46] Frederic Crevecoeur and Konrad P Kording. Saccadic suppression as a perceptual consequence of efficient sensorimotor estimation. *Elife*, 6:e25073, 2017.
- [47] Alessandro Benedetto and Paola Binda. Dissociable saccadic suppression of pupillary and perceptual responses to light. *Journal of neurophysiology*, 115(3):1243–1251, 2016.
- [48] Michael R MacAskill, Richard D Jones, and Tim J Anderson. Saccadic suppression of displacement: Effects of illumination and background manipulation. *Perception*, 32(4):463–474, 2003.
- [49] Mark R Diamond, John Ross, and Maria C Morrone. Extraretinal control of saccadic suppression. *Journal of Neuroscience*, 20(9):3449–3455, 2000.
- [50] GG Landis JRKoch. The measurement of observer agreement for categorical data. *Biometrics*, 33(1):159–74, 04 1977.
- [51] A Terry Bahill and Lawrence Stark. Neurological control of horizontal and vertical components of oblique saccadic eye movements. *Mathematical Biosciences*, 27(3-4):287–298, 12 1975.
- [52] Dillon Lohr and Oleg V Komogortsev. Eye know you too: Toward viable end-to-end eye movement biometrics for user authentication. *IEEE Transactions on Information Forensics and Security*, 17:3151–3164, 2022.
- [53] Supratim Gupta and Aurobinda Routray. Estimation of saccadic ratio from eye image sequences to detect human alertness. In *2012 4th International Conference on Intelligent Human Computer Interaction (IHCI)*, pages 1–6. IEEE, 2012.